NOTES AND CORRESPONDENCE

Investigating Spatial Downscaling of Satellite Rainfall Data for Streamflow Simulation in a Medium-Sized Basin

SAYMA RAHMAN AND AMVROSSIOS C. BAGTZOGLOU

Department of Civil and Environmental Engineering, University of Connecticut, Storrs, Connecticut

FAISAL HOSSAIN AND LING TANG

Department of Civil and Environmental Engineering, Tennessee Technological University, Cookeville, Tennessee

LANCE D. YARBROUGH AND GREG EASSON

Department of Geological Engineering, University of Mississippi, University, Mississippi

(Manuscript received 8 July 2008, in final form 23 January 2009)

ABSTRACT

The objective of this study was to investigate spatial downscaling of satellite rainfall data for streamflow prediction in a medium-sized (970 km^2) river basin prone to flooding. The spatial downscaling scheme used in the study was based on the principle of scale invariance. It reproduced the rainfall variability at finer scales while being conditioned on the large-scale rainfall. Two Tropical Rainfall Measuring Mission (TRMM)-based real-time global satellite rainfall products were analyzed: 1) the infrared (IR)-based 3B41RT product available at 1 hourly and 0.25° scales and 2) the combined passive microwave (PMW) and IR-based 3B42RT product available at 3 hourly and 0.25° scales. The conceptual Hydrologic Engineering Center-Hydrologic Modeling System (HEC-HMS) was used for the simulation of streamflow. It was found that propagation of spatially downscaled satellite rainfall in the hydrologic model increased simulation uncertainty in streamflow as rainfall grid scales became smaller than 0.25°. The streamflow simulation uncertainty for satellite downscaling was found to be very similar to that for ground validation Next Generation Weather Radar (NEXRAD) downscaling at any given scale, indicating that the effectiveness of the spatial downscaling scheme is not influenced by rainfall data type. Closer inspection at the subbasin level revealed that the limitation of the selected spatial downscaling scheme to preserve the mean rainfall intensity for irregularly sized drainage units was responsible for the increase in simulation uncertainty as scales became smaller. Although the findings should not be construed as a generalization for spatial downscaling schemes, there is a need for more rigorous hydrometeorological assessment of downscaled satellite rainfall data prior to institutionalizing its use for real-time streamflow simulation over ungauged basins.

1. Introduction

Spatial downscaling is a technique for disaggregation of coarse-resolution data for applications where finer resolution input is required. Given the sparseness of in situ networks for rainfall measurement and the coarseness associated with the ''effective'' scale (spacing) of point rainfall observations (~25–100 km), spatial downscaling techniques have historically found widespread use for rainfall disaggregation in hydrologic modeling applications that require finer spatial resolutions (~1–5 km). Satellite rainfall data in particular have benefited from spatial downscaling techniques (Hossain and Lettenmaier 2006), because most rainfall products from spaceborne platforms are typically provided at large space–time scales suitable for coarse-scale meteorological applications, such as climatologic analysis, or water balance studies (Shepherd et al. 2002).

Corresponding author address: Dr. Faisal Hossain, Department of Civil and Environmental Engineering, 1020 Stadium Drive, Box 5015, Tennessee Technological University, Cookeville, TN 38505-0001.
E-mail: fhossain@tntech.edu

DOI: 10.1175/2009JHM1072.1

As an example, the satellite rainfall algorithm called Precipitation Estimation from Remotely Sensed Information using Artificial Neural Networks (PERSIANN; Sorooshian et al. 2000) estimates 0.04°, half-hourly rainfall by using the Climate Prediction Center merged infrared (IR) dataset (Janowiak et al. 2001) at full resolution and disaggregating the passive microwave (PMW) estimates from 0.12° grids with guidance from the IR field (Hong et al. 2005).

Although there are several approaches for downscaling rainfall, one of the most common technique is based on the concept of ''scaling,'' or relating the properties associated with the rainfall process at one scale to those at a finer scale (see, e.g., Perica and Foufoula-Georgiou 1996a; Venugopal et al. 1999; Bindlish and Barros 2000; Ahrens 2003; Ferraris et al. 2003, among others). Most spatial downscaling schemes honor certain characteristics during the disaggregation process. These characteristics include the (i) preservation of the rainfall intensity at the starting (or another specified) spatial scale; (ii) stochastic nature of yielding equiprobable realizations; and (iii) simulation of the expected variance at downscaled resolution based on the scaling property of rainfall. For a useful summary on the various classifications of spatial downscaling techniques, refer to Ferraris et al. (2003).

Our review of current literature indicates that most spatial downscaling schemes, to the best of our knowledge, may not have been assessed of their physical implications on hydrologic modeling and, in particular, for streamflow simulation based on satellite rainfall data (Nykanen et al. 2001). One physical aspect that warrants a closer inspection is the implication of ''redistribution'' (in space) of the rainfall because of spatial downscaling on overland runoff simulation accuracy. Herein, redistribution refers to the spatial ''spread'' of downscaled rainfall data when compared to the ''true'' field (assuming that the true rainfall field at the downscaled resolution is known a priori). For example, it is possible statistically for a downscaling technique to register rain in some grid boxes (or pixels) that are supposed to be dry (nonrainy) at the downscaled resolution. Vice versa, some rainy grid boxes may be identified as zero rainfall grid boxes by the technique at the downscaled resolution.

A question that therefore appears largely unexplored is, although spatial downscaling schemes preserve the mean and mimic the expected variance of the rainfall intensity, is that generally acceptable for stream flow simulation based on downscaled satellite rainfall data at smaller scales? The effect of not adequately capturing the small-scale rainfall variability (i.e., second- and higher-order moments) and the propagation of this variability via the nonlinear hydrologic equations may result in significant biases of the predicted variables at scales larger than the scale of the dominant rainfall variability (Nykanen et al. 2001; Bindlish and Barros 2000).

In the long run, gaining insights on the above question is particularly important because of the current community-wide agenda on the Program to Evaluate High Resolution Precipitation Products (PEHRPP) and the Global Precipitation Measurement (GPM) mission. PEHRPP is an effort led by the International Precipitation Working Group (IPWG) to evaluate the quality of currently available high-resolution satellite rainfall products (Ebert et al. 2007). The GPM mission, in collaboration with major international space partners, will represent a unique constellation of rain-measuring satellites comprising PMW sensors (Smith et al. 2007), providing almost real-time rainfall information on a global basis. GPM is currently scheduled for launch in 2013 (available online at http://gpm.gsfc.nasa.gov).

Naturally, satellite rainfall data will become more widely available at smaller scales with a better understanding of the associated uncertainty in the future. A logical progression to this anticipated scenario requires us to take a closer look at spatial downscaling and identify the role downscaling techniques should play for agendas like PEHRPP and GPM. There are no obvious answers today to questions such as the following: will there be as much a need for spatial downscaling as there is today; or, if satellite rainfall data are characterized by scale-dependent uncertainty, what role does downscaling play in transforming this uncertainty at the disaggregated resolution? Hence, it is important that we begin a detailed investigation of downscaling technique and identify the physical implications for streamflow prediction.

The objective of this study is, therefore, to investigate spatial downscaling for satellite-based streamflow simulation in anticipation of the proposed GPM mission. A secondary objective is to investigate the influence of various rainfall types in downscaling. Because most spatial downscaling schemes are different in algorithm formulation (Ferraris et al. 2003), findings from this study are limited to the specific scheme investigated herein (described in section 2). Nevertheless, one of our goals is to generalize our study toward recommendations on how spatial downscaling schemes should be assessed for disaggregation of satellite rainfall data in light of GPM and PEHRPP. Two TRMM-based real-time global satellite rainfall products, considered as forerunners to GPM products, are analyzed: 1) the IR-based 3B41RT product, available at 1 hourly and 0.25° scales; and 2) the combined PMW- and IR-based 3B42RT product, available at 3 hourly and 0.25° scales. The study is organized as follows: section 2, provides a brief description of study region, data, hydrologic

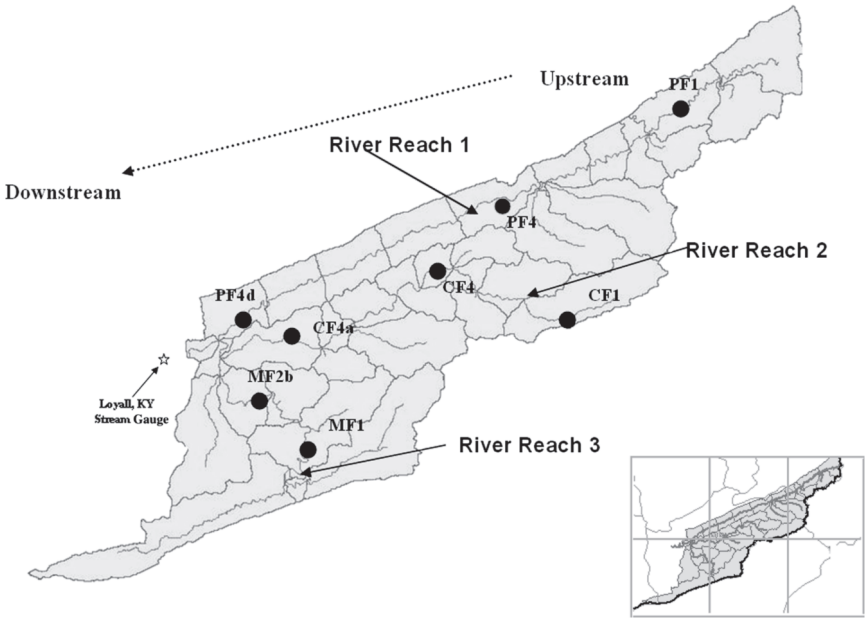

FIG. 1. The UC River basin and the river network. Circles and arrows indicate the three river reaches and the location of selected subbasins for closer inspection of the rainfall-runoff relationship as a function of disaggregated scale. Star denotes the stream gauge located close to the basin outlet in Loyall. The inset shows the six satellite rainfall grid boxes at 0.25° scale.

model, and the spatial downscaling technique. Section 3 describes the methodology used to gauge the effectiveness of spatial downscaling for streamflow prediction. Section 4 presents the results of the downscaling effectiveness, followed by a closer inspection for eliciting physical insights. Finally, section 5 provides the conclusions and future extensions of this study.

2. Study area, data, and models

a. Study area

The region of interest for this work is the upper 970 km^2 of the Upper Cumberland (UC) River basin in southeastern Kentucky (Fig. 1). The UC basin is mainly a mountainous area (i.e., elevation ranges from 150 to 1200 m MSL) that lies in the Eastern Mountain Coal Fields region. The underlying rock formations are primarily sandstone, shale, and siltstone. A major part of it (80.13%) is forest land, whereas only 8.20% is urban area. Cropland and pasture makeup 11.15%, and the combined lakes and reservoirs occupy 0.52%. The UC River basin has been subject to frequent flooding. In April 1977, for example, record rainfall caused severe flooding and damages, which then led to the declaration of federal disaster areas by President Jimmy Carter. More recently, major flooding took place in 2002 (Harris et al. 2007).

b. Data

Three rainfall events of varying characteristics (in terms of duration, pattern of intensity, season, and streamflow dynamics) are selected for investigation of spatial downscaling. All three events generated peak flows ranging between 10 000 and 50 000 cubic feet per second (cfs). Table 1 summarizes the statistical characteristics of the rainfall and the ensuing streamflow hydrograph for these three rain events. The reference rainfall data considered as ground validation (GV) data are Next Generation Weather Radar (NEXRAD) radar rainfall data (Fulton et al. 1998) cropped over the basin area. To minimize the uncertainty of the GV data in our investigation, we used the National Centers for Environmental Prediction's (NCEP) 4-km stage IV NEXRAD rainfall data that is adjusted to gauges and conveniently available as a quality-controlled data mosaic over the United States (Lin and Mitchell 2005).

Typically, the period from February to March is the wettest in the Cumberland region of eastern Kentucky (Gaffin and Lowery 2008). Hence, the first two events (events 1 and 2) that took place on 10–25 March 2002 and 13–23 February 2003, respectively, resulted in high floodlike peaks. Event 3, on the other hand, took place during the considerably drier month of July of 2002, with a higher frequency of low rain rates. A month-long period is considered for event 3 to assess the performance

TABLE 1. Summary of rainfall events studied.

	Event 1	Event 2	Event 3
Date	10–25 Mar 2002	13–22 Feb 2003	1–31 Jul 2002
Total rainfall accumulation (mm)	137.6	172.85	89.59
Duration (days)	16	10	31
Mean rainfall rate (mm h^{-1})*	0.36	0.725	0.124
Standard deviation of rainfall rate (mm h^{-1})*	1.34	1.53	0.327
Percentage of 1-h periods with rain	29.68	60.41	38.57
Maximum streamflow (cfs)	29 600	29 208	7190.0
Runoff volume (cfs day^{-1})	41 879	44 094	36 324

* Computed over the whole duration of the event.

of spatial downscaling during longer periods of rainfall hiatus (or low rain) when efficient water management is critical in the southeastern United States.

In terms of storm characteristics and heavy precipitation climatology, the study region is frequently subject to orographic effects throughout the year. In general, most synoptic weather systems in this region generally move from west to east, with cold fronts aligned southwest to northeast. The Gulf of Mexico also contributes to high moisture content, particularly across southern regions of the study area during early spring (Troutman et al. 2008). Figure 2 shows the rainfall hyetographs, while the ensuing streamflow hydrographs are shown in Fig. 3.

The observed streamflow was measured at the outlet of the basin in Loyall, Kentucky, at the U.S. Geological Survey streamflow gauge 03401000 (Fig. 1). This gauge was operated in cooperation with the U.S. Army Corps of Engineers (USACE; Harris et al. 2007).

The National Aeronautics and Space Administration's (NASA) real-time satellite rainfall data products from PMW-calibrated IR and merged PMW–IR estimates and labeled as 3B41RT and 3B42RT, respectively, are used as satellite rainfall input for spatial downscaling. The products 3B41RT and 3B42RT are produced at 0.25° with hourly and 3-hourly temporal resolution, respectively (Huffman et al. 2007). These are globally available on a near-real-time basis (available online at ftp://trmmopen.gsfc.nasa.gov, or at http://precip.gsfc.nasa.gov). These products are expected to act as pathfinders to a hydrologically more optimal rainfall product in the GPM era of post-2013. Currently, NASA employs these products for the development of a real-time and global flood and landslide detection system (Hong et al. 2007). Hence, it is likely that future satellite rainfall products from the GPM era will evolve from these products.

c. Hydrologic model

The hydrologic model used for streamflow simulation was the Hydrologic Engineering Center's (HEC) Hydrologic Modeling System (HMS), version 3.0. HEC-HMS is a conceptual hydrologic model system that simulates the rainfall-runoff processes of dendritic watershed systems. Each modeling run comprises three components: the basin model, the meteorological model, and the control specifications. In the basin model, the size, infiltration method, rainfall-runoff routing method, base flow, and other physical parameters are specified. The precipitation and evapotranspiration parameters are specified in the meteorological model, and the dates and time step of the model are selected in the control specifications.

Because of frequent disastrous flooding in the region, the USACE Nashville District (available online at http://www.lrn.usace.army.mil) had recently undertaken a Section 202 Flood Reduction project on the UC River

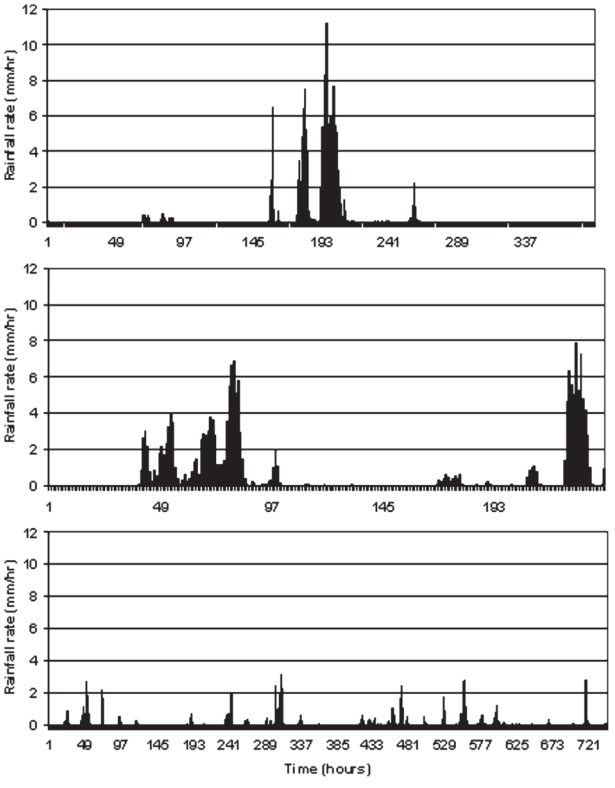

FIG. 2. Rainfall hyetographs for (top to bottom) events 1, 2, and 3.

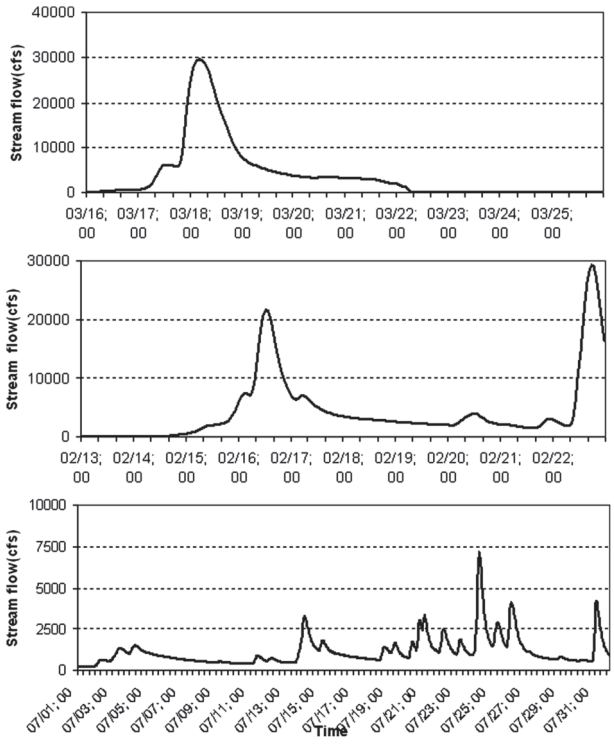

FIG. 3. Observed streamflow hydrographs and date range for the three events [(top) 1: 10–25 Mar 2002; (middle) 2: 13–22 Feb 2003; and (bottom) 3: 1–31 Jul 2002].

basin. The model, with the outlet at Loyall, Kentucky, is calibrated using the Soil Conservation Service (SCS) Curve Number method for calculating surface runoff. For modeling of runoff, the watershed is subdivided into 31 subbasins, each connected by one of the three major river reaches and junctions and having an area in the ranges of 15–50 km^2 (Fig. 1). The other components selected for use in the HEC-HMS model are the Modified Clark (ModClark) overland flow transformation (Kull and Feldman 1998) and Muskingum–Cunge river routing (Barry and Bajracharya 1995). NEXRAD rainfall is used as input for calibrating model parameters [refer to HEC (2000) for further details on HEC-HMS usage]. Details of the hydrologic model setup and calibration for the UC basin are described in Harris et al. (2007) and Harris and Hossain (2008).

d. Spatial downscaling scheme

This study used the wavelet-based spatial downscaling scheme developed by Perica and Foufoula-Georgiou (1996b). This scheme has the ability to reproduce the rainfall variability at finer scales while being conditioned on the large-scale rainfall average and physical properties of prestorm conditions. The scheme is developed on the basis of two hypotheses for midlatitude mesoscale convective systems (MCS) as follows: 1) standardized rainfall fluctuations (defined via a Haar wavelet transform) exhibit simple scale over the mesoscale and 2) statistical scaling parameters of rainfall fluctuation are related to convective available potential energy (CAPE), which measures convective instability of prestorm environment (Perica and Foufoula-Georgiou 1996a). Herein, rain fluctuation refers to the variation in space.

Whereas most rainfall downscaling schemes have the ability to predict the small-scale rainfall variability, the chosen technique of Perica and Foufoula-Georgiou (1996b) has two particular advantages: 1) the statistical characterization of downscaling applies over a range of scales with a single parameter H that defines scale invariance and 2) the value of H is linked to the CAPE of the prestorm environment. Unlike many downscaling techniques, therefore, this scale invariance parameter allows parsimony in the downscaling model and a convenient pathway to leverage information on a physical variable (CAPE) that is computed in most mesoscale models.

The CAPE–H relationship as reported in Perica and Foufoula-Georgiou (1996b) is not used for the derivation of the scaling parameter H, because the use of a mesoscale model to estimate a representative CAPE is beyond the scope of this study. Rather, the scaling parameter H is estimated from the available rainfall data. A statistical scaling analysis is performed wherein the slope of the line for standard deviation versus scale (on a log-log scale) yielded an estimate for H. Spatial downscaling is then performed using the inverse Haar wavelet transform in the manner outlined in Perica and Foufoula-Georgiou (1996b). The derivation of H from data is described as follows.

In this study, the downscaling code first computed the standard deviation of rainfall in each of the three directions (x, y, and diagonal) at three scales—0.25°, 0.50°, and 1.0°—using satellite rainfall data provided to the scheme over a larger 64 × 64 gridded domain around the study region. For example, actual 3B42RT or 3B41RT data pertaining to the storm periods is used for computation of the scaling parameters representative of the specific satellite rainfall product being investigated. For the latter two scales, data are aggregated (upscaled) from the native scale of 0.25°. Next, the standard deviation for each direction is plotted on a log-log scale against the spatial scale to fit a straight line. The slope of the line then yielded the H for the direction concerned, which is then used for representing variability in downscaled data.

For this study, the downscaling scheme is used to generate finer-scale data at three ''down scales'' (0.125°, 0.0625°, and 0.03125°) from the native scale (0.25°). The scales are equivalent to 12.5, 6.25, 3.125, and 25.0 km,

respectively. A threshold value of 0.1 mm h^{-1} is used in the downscaling scheme for distinguishing rainy from nonrainy areas. According to Perica and Foufoula-Georgiou (1996b), threshold values ranging from 0.1 to 0.25 mm h^{-1} are recommended. The scaling parameter H is calculated for each satellite product using as input rainfall data from a much larger (64×64 grid domain) field at the native scale of 0.25° from the midlatitude regions of the United States. The data at 0.25° scale is first upscaled to 0.50°, 1.0°, and 2.0° and then the best-fit slope value is derived. The downscaled data are then propagated through the streamflow model (discussed in section 3). Prior to this study, the downscaling scheme was thoroughly verified to ensure that the mean rainfall intensity at disaggregated scales was preserved consistently. Although details on the verification of the downscaling scheme for the UC River basin may be found in Rahman (2008), we provide a summary of essential features of quality assurance and quality control (QA/QC) of the downscaling scheme in the appendix.

3. Methodology

a. Specific approach

The specific approach of the study is first summarized in Fig. 4. Satellite rainfall data at 0.25° is downscaled to three smaller scales (0.125°, 0.0625°, and 0.03125°). Then, 200 Monte Carlo (MC) realizations of disaggregated rainfall data are created. The mean and $\pm\sigma$ (standard deviation) of the MC realizations are then propagated through HEC-HMS for the derivation of streamflow simulation uncertainty. This had two advantages. First, the Perica and Foufoula-Georgiou (1996b) scheme is a purely "spatial" downscaling scheme with no explicit accommodation of the autocorrelation of the rainfall system. Thus, the mean and standard deviation of 200 MC realizations yielded downscaled rainfall fields at each time step that do not undermine the inherent persistence of rainfall within the event as a result of the random nature of the stochastic downscaling. Second, in the current scheme of operations, HEC-HMS has no provision for executing automatic Monte Carlo simulation. Each realization needs to be propagated manually. The propagation of only three streaks (mean and $\pm\sigma$), therefore, made our investigation manageable in terms of time and effort. We have also verified that the propagation of the three streaks of disaggregated rainfall are, indeed, equivalent to propagating each realization and deriving the mean and $\pm\sigma$ in streamflow. Evidence of this equivalency is shown in the appendix. Finally, the NEXRAD GV data, available at the native scale of 0.04° (remapped from NCEP 4-km earth parallel grids), is aggregated to 0.25° and then downscaled to the three

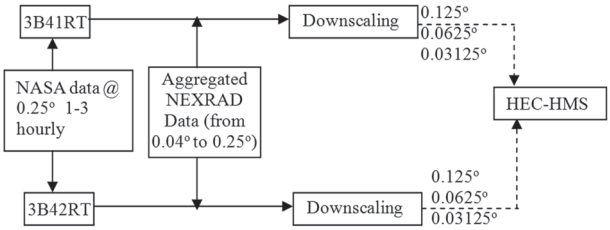

FIG. 4. General approach used in the study for investigating the effectiveness of spatial downscaling of satellite rainfall for streamflow prediction.

smaller scales as well. The objective of applying upscaled NEXRAD data to spatial downscaling is to distinguish the response on streamflow prediction as a function of data type (satellite versus ground validation data) and to minimize model calibration issues (since HEC-HMS model parameters were calibrated using NEXRAD data).

In the current HEC-HMS setup, there are 31 subbasins for the UC River basin (Fig. 1). Each subbasin requires areal-averaged rainfall as a time series for simulation of flow at the subbasin outlet. To calculate the subbasin-averaged rainfall, the percentage area of each subbasin that lies in a grid box is identified for each scale (0.25°, 0.125°, 0.0625°, and 0.03125°). Figure 5 illustrates the concept for the four spatial scales. At 0.25° resolution, the subbasin area falls under two satellite grid boxes (see upper-left corner of Fig. 5). By calculating the relative percentage of area for each color, the weight that needs to be assigned to the rainfall value of each satellite grid box to compute the areal average of rainfall for the subbasin is determined. As the scale gets smaller, more downscaled satellite grid boxes overlay a given subbasin and relative weights need to be identified for each one of them accordingly. If there are n grid boxes overlaying a given subbasin, then the areal-average rainfall for that subbasin is calculated as

$$\text{Average rainfall at a time step} = \sum_{i=1}^{n} w_i R_i, \qquad (1)$$

where w_i is the relative weight for grid box i, and R_i is the satellite rainfall for grid box i.

b. Metrics for investigating downscaling

The three MC rainfall scenarios—mean, mean $-\sigma$, and mean $+\sigma$—derived from 200 downscaled realizations that are propagated through HEC-HMS yields corresponding uncertainty limits in streamflow simulation (for each event). The metrics *exceedance probability* (EP) and *uncertainty ratio* (UR) are used to assess the implication of downscaling on flood prediction. These metrics are defined as follows:

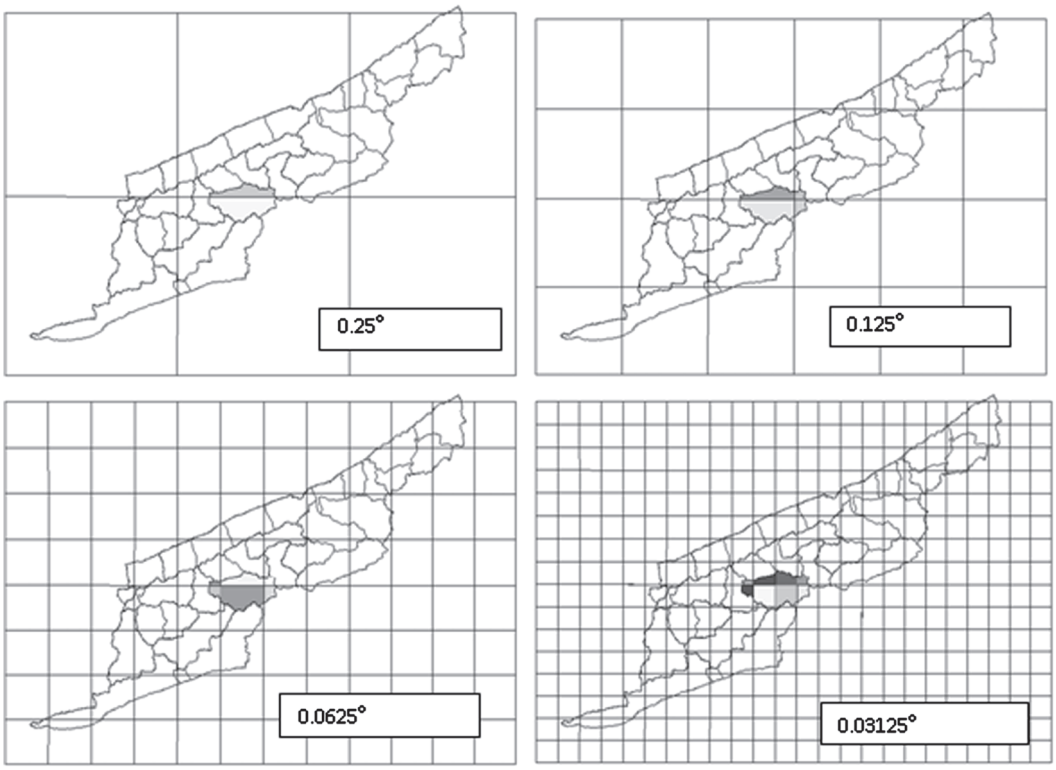

FIG. 5. GIS map (shape files) of satellite grid boxes (at four scales) overlaid on subbasin maps. For each satellite scale, the percentage area of a given subbasin in a satellite grid box is identified (refer to the gray-shaded areas for each grid box). These percentages act as weights to calculate the areal-average rainfall for the subbasin from satellite rainfall downscaled data.

$$\mathrm{EP} = \frac{\text{Number of times observed streamflow exceeds the uncertainty limits}}{\text{Total number of timesteps}} \quad \text{and} \tag{2}$$

$$\mathrm{UR} = \frac{\text{Uncertainty in runoff volume simulation (beween uncertainty limits)}}{\text{Observed runoff volume}}. \tag{3}$$

To normalize the EP and UR value at a given scale of satellite data to that obtained using NEXRAD GV data, two more metrics are defined. These are expressed as follows:

$$\text{EP ratio} = \frac{\mathrm{EP}_{\mathrm{SATELLITE}}}{\mathrm{EP}_{\mathrm{NEXRAD}}} \quad \text{and} \tag{4}$$

$$\text{UR ratio} = \frac{\mathrm{UR}_{\mathrm{SATELLITE}}}{\mathrm{UR}_{\mathrm{NEXRAD}}}. \tag{5}$$

In the above equations (4 and 5), the denominator represents the EP and UR values that are obtained by applying downscaled NEXRAD data derived from aggregated NEXRAD data (at 0.25°). The advantage of using these two ratio metrics is that they provide performance evaluation of satellite rainfall data relative to the more conventional scenario of using GV rainfall data for gauged river basins. Hence, an EP ratio of 0 would mean that the entire observed hydrograph is enveloped by the simulated error bounds. A value of 1 would signify that the probability of the observed flow exceeding the simulated error bound for satellite data is the same as that for NEXRAD data.

The Nash–Sutcliffe efficiency performance measure (Nash and Sutcliff 1970) is also computed for this study:

$$E_{\mathrm{NS}} = \left(1 - \frac{\sigma_e^2}{\sigma_{\mathrm{obs}}^2}\right). \tag{6}$$

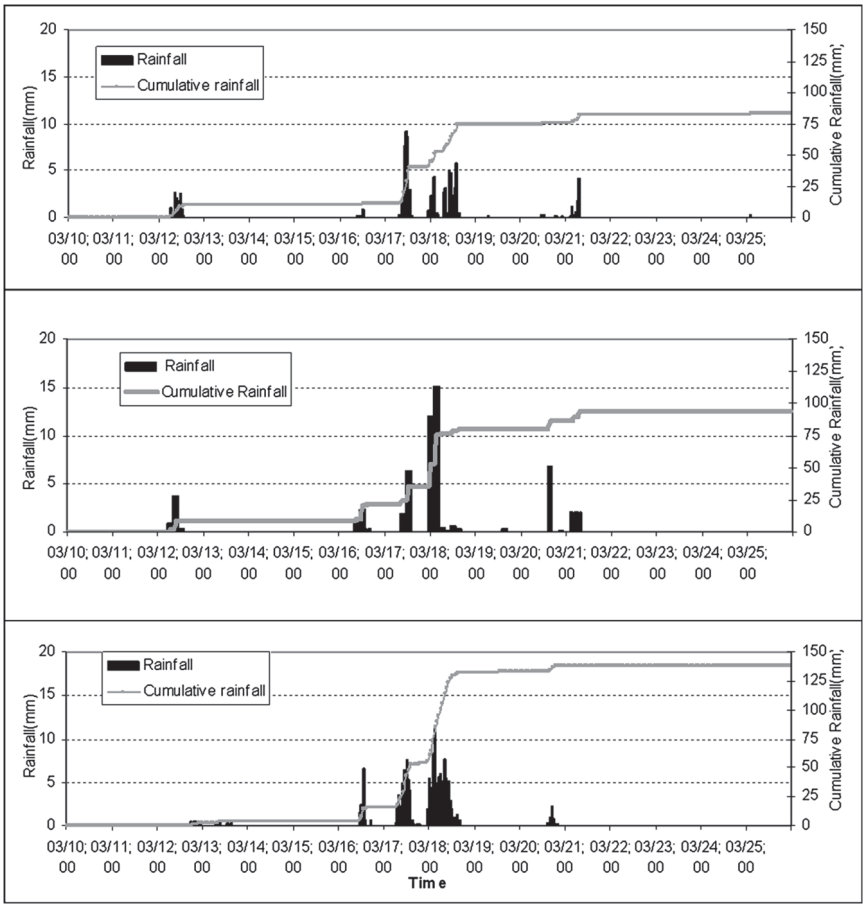

FIG. 6. Basin-averaged rainfall hyetographs for event 1 for (top to bottom) 3B41RT, 3B42RT, and NEXRAD.

In Eq. (6), subscripts *e* and obs refer to errors and observations, respectively. Absolute values of relative errors (%) in time to peak, peak runoff, and runoff volume are also computed. Herein, efficiency and the relative errors are calculated with respect to the satellite-derived hydrograph obtained by propagating the mean of the 200 MC realizations.

4. Results and discussion

a. Satellite data adjustment

Because the focus of the study is solely on investigating the spatial downscaling, an effort is made to remove as much bias as possible from actual satellite data prior to downscaling. As an example, Fig. 6 shows the cumulative hyetographs of event 1 for NEXRAD, 3B41RT, and 3B42RT rainfall over the UC basin. The satellite rainfall products are found to underestimate rainfall by considerable margins when compared to NEXRAD for event 1. Typically, it is observed that both satellite products estimate rainfall for a given event by a factor ranging from 0.5 (underestimation) to 2.5 (overestimation). All satellite rainfall data is, therefore, bias-adjusted (using NEXRAD as reference) accordingly to make satellite-derived hydrograph mimic as closely as possible the observed streamflow. In the post-GPM era, this bias adjustment may be considered equivalent to the research-level 3B42 V6 product that is planned for real-time generation based on dynamic bias adjustment (Huffman et al. 2007). The Figs. 7a,b demonstrate the effectiveness of this bias adjustment for event 1 and event 2, respectively, where reasonably accurate streamflow simulation is obtained using the bias-adjusted satellite data. Further details of bias adjustment can be found in Rahman (2008).

b. Propagation of downscaled rainfall data in HEC-HMS

Figures 8a,b show the streamflow simulation uncertainty for event 1 using downscaled 3B42RT and NEXRAD data, respectively. Figure 9 demonstrates the streamflow simulation uncertainty for event 2 (top)

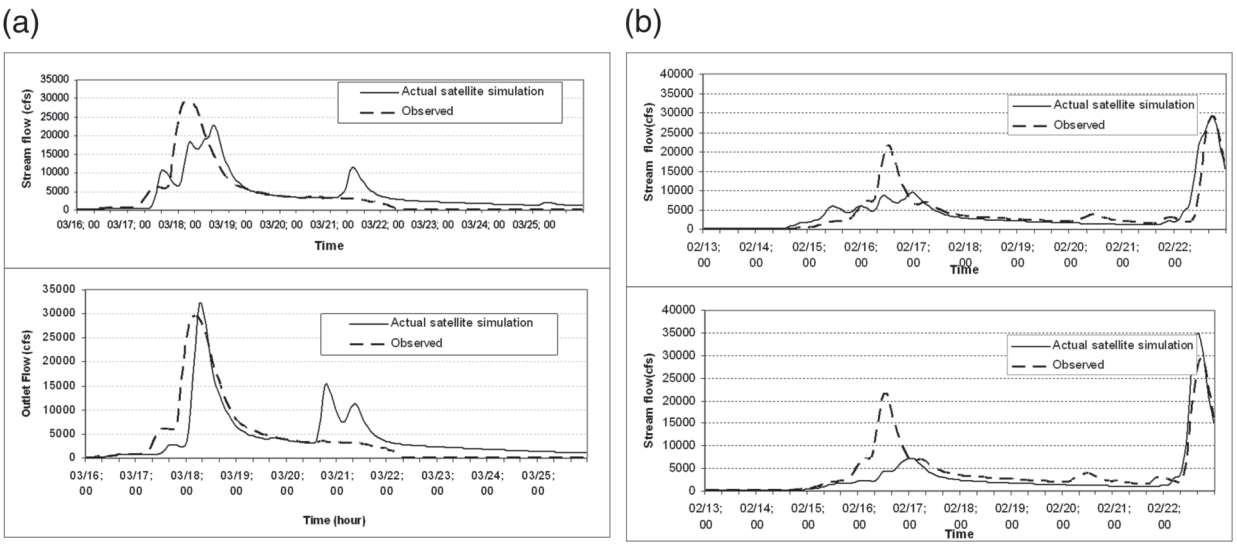

FIG. 7. (a) Stream flow simulation for event 1 using bias-adjusted satellite rainfall data (top) 3B41RT and (bottom) 3B42RT at native scale of 0.25° (no downscaling). (b) Same as (a) but for event 2.

and event 3 (bottom) using downscaled 3B42RT data at the 0.0625° resolution. (For performance metrics at other resolutions and products, refer to Tables 3 and 4.)

The most common trend seen for all events (Figs. 8 and 9) is that streamflow simulation uncertainty systematically increases with each successive level of downscaling. This effect is also found to be independent of the data type, because a similar pattern is also observed for NEXRAD for event 1 (see Fig. 8b). For all three events, it appears that spatial downscaling of satellite

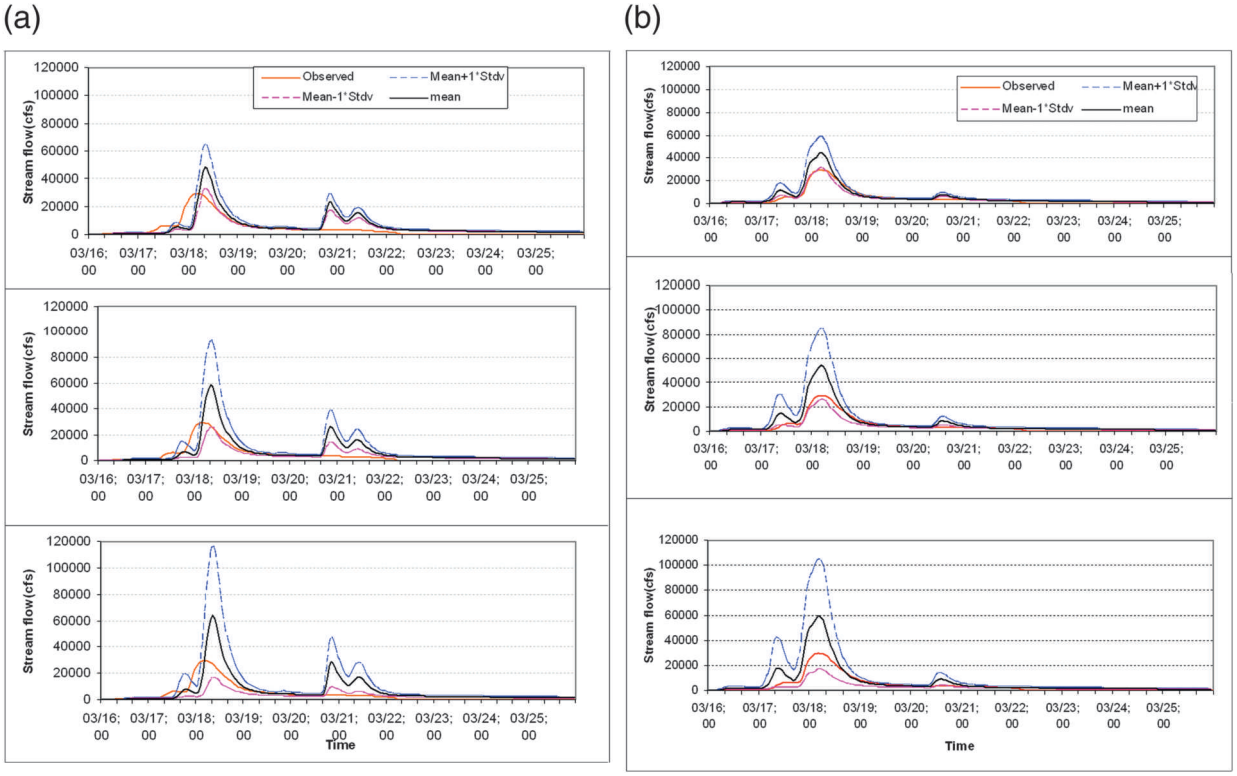

FIG. 8. (a) Stream flow simulation uncertainty for event 1 using downscaled 3B42RT data at (top to bottom) 0.125°, 0.0625°, and 0.03125°. (b) Same as (a) but for downscaled NEXRAD.

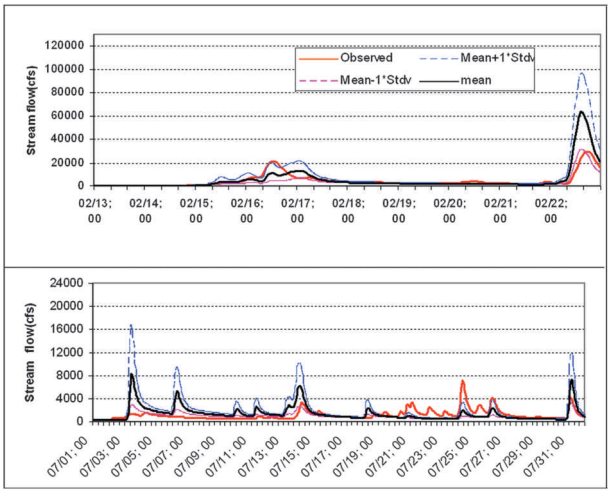

FIG. 9. Stream flow simulation uncertainty for (top) event 2 and (bottom) event 3 using downscaled 3B42RT data at −0.0625° resolution.

rainfall data does not categorically yield an improvement (in terms of reduced uncertainty or more accurate simulation) at the next smaller downscaled resolution (when compared to the simulation obtained with native scale data). Simulation uncertainty appears to increase consistently (in terms of width of error bars) as scales become smaller for HEC-HMS.

Tables 2 and 3 summarize quantitatively the performance metrics using NEXRAD and satellite data, respectively, for event 1. Product wise, more accurate performance is generally obtained with downscaled PMW-IR 3B42RT than with IR 3B41RT data for the temporal aspects of hydrograph simulation (such as lower EP and EP ratios in Table 3). The relative error in time to peak is considerably lower for 3B42RT (for events 1 and 3). For other features (such as error in runoff volume or peak runoff), simulation uncertainty of 3B42RT and 3B41RT seem statistically quite similar. For both products, a considerable worsening of efficiency of simulation is observed at scales smaller than 0.125°. The uncertainty width (UR) appears to almost double at each successively smaller scale. In terms of UR, the simulation uncertainty using downscaled 3B41RT or 3B42RT is found to be very similar to that obtained from NEXRAD (UR ~ 1.00–1.10). The EP ratio is, however, considerably higher. This indicates that a probabilistic flood warning derived from downscaled satellite rainfall data at any given time step is likely to be considerably less certain compared to that derived from NEXRAD data. Finally, in Table 4, the quantitative measures of performance metrics for events 2 and 3 further confirm the observation for event 1 that satellite downscaling increases streamflow prediction uncertainty.

c. *How accurate is the preservation of rainfall's spatial structure during spatial downscaling?*

Generally speaking, the assumption, that as the scale (grid size) is reduced, the uncertainty of streamflow prediction would decrease, should be considered a valid one. In an earlier study, Ahrens (2003) reports that downscaling of rainfall fields with 16-km grid spacing to fields with 1-km grid spacing can result in about a 5%–10% improvement in the simulation accuracy of runoff for an alpine watershed of comparable size as the UC basin. Other studies, such as the Bindlish and Barros (2000) study, also reported similar findings using downscaled model rainfall data for studying the hydrologic response at the subgrid scale. So, the observations reported in this study on spatial downscaling systematically increasing simulation uncertainty are counterintuitive at first. To achieve a more physical understanding of the observations from a hydrologic standpoint, a closer inspection of the rainfall-runoff process is undertaken. This is described next.

One physical aspect that needs to be studied is the nature of variability (in space) of the rainfall due to spatial downscaling and its consequent implications on overland runoff simulation uncertainty. Herein, variability may refer to the spatial "offset" of downscaled rainfall data from the true field (assuming that the true field is known a priori). For example, some areas may register rain as having spread out on actually dry regions, whereas other actually rainy areas may exhibit zero rainfall at the downscaled resolution. Overall, this

TABLE 2. Summary of performance metrics for NEXRAD for all error propagation scenarios for event 1.

	0.25° (actual data)	0.125° (downscaled)	0.0625° (downscaled)	0.03125° (downscaled)
Efficiency	0.832	0.318	−0.0656	0.236
EP	N/A	0.262	0.0417	0.0167
UR	N/A	0.724	1.446	2.163
Error in peak runoff (%)	0.20	49.774	82.973	100.346
Error in peak runoff time (hr)	0	0	0	0
Error in runoff volume (%)	1.4	36.536	53.547	63.208

TABLE 3. Summary of performance metrics for all error propagation scenarios using 3B41RT and 3B42RT for event 1.

Scale product		0.25° actual	0.125°	0.0625°	0.03125°
Efficiency	3B41RT	0.60	0.539*	0.303*	0.132*
	3B42RT	0.64	0.232*	0.040*	0.245*
EP	3B41RT	N/A	0.933	0.817	0.40
	3B42RT	N/A	0.921	0.767	0.292
UR	3B41RT	N/A	0.793	1.603	2.352
	3B42RT	N/A	0.749	1.493	2.175
EP	3B41RT	N/A	3.561	19.592	23.952
	3B42RT	N/A	3.515	18.393	17.485
UR	3B41RT	N/A	1.095	1.109	1.087
	3B42RT	N/A	1.034	1.032	1.006
Error in peak runoff (%)	3B41RT	22.71	5.64*	27.74*	38.87*
	3B42RT	8.84	63.68*	97.70*	115.69*
Error in peak runoff time (hr)	3B41RT	12.0	11.0*	11.0*	11.0*
	3B42RT	3.0	4.0*	4.0*	4.0*
Error in runoff volume (%)	3B41RT	11.03	50.45*	69.10*	76.99*
	3B42RT	12.21	47.55*	62.48*	70.09*

* Computed from the simulation obtained from the mean of 200 realizations.

offset may be called a redistribution phenomenon (as already discussed in section 1) and is shown in Figure 10. A 32×32 rainfall field is upscaled to a 16×16 field and then subsequently downscaled back to the 32×32 field using the Perica and Foufoula-Georgiou (1996b) model. The scaling coefficients are computed from the original and upscaled fields. For one random realization, the following features of downscaling are clearly apparent from Fig. 10: 1) rainy grid boxes can sometimes be predicted as nonrainy; 2) nonrainy grid boxes can sometimes be predicted as rainy; and 3) there can be significant bias in the rainfall estimation over many rainy areas, even when the mean rainfall intensity remains constant over the entire domain. Rahman (2008) reported that the downscaling scheme of Perica and Foufoula-Georgiou (1996b) can wrongly classify a rainy (nonrainy) grid box as nonrainy (rainy) about 5%–10% of the time.

Some of the features reported above are not uncommon for downscaling schemes. Most spatial downscaling schemes were developed in response to disaggregating the coarse-resolution rainfall output from the numerical weather prediction (NWP) or global circulation models (GCMs) for use in macroscale hydrologic models (Nijssen et al. 2001). Therein, the typical performance methods used for assessing the accuracy of disaggregation schemes pertained mostly to fractional coverage of rain, conditional rain-rate distribution, or empirical semivariograms (Perica and Foufoula-Georgiou 1996b). These methods, although being useful, are not hydrologically sufficient to constrain the generation of overland runoff at smaller scales. Multiple spatial structures of rainfall over land (and hence multiple overland runoff responses) are possible for a single fractional coverage numeric value, empirical semivariogram, or conditional rain rate

TABLE 4. Same as Table 3 but for events 2 and 3.

Scale product		0.25° actual events		0.125°		0.0625°		0.03125°	
Efficiency	3B41RT	0.78	−0.03	0.37*	−1.00*	−0.47*	−1.80*	−1.00*	−2.10*
	3B42RT	0.68	−0.19	0.37*	−1.20*	−0.25*	−0.16*	−0.40*	−1.06*
EP	3B41RT	N/A	N/A	0.59	0.46	0.53	0.25	0.43	0.15
	3B42RT	N/A	N/A	0.82	0.83	0.67	0.69	0.47	0.26
UR	3B41RT	N/A	N/A	0.74	0.41	1.60	0.80	2.49	1.14
	3B42RT	N/A	N/A	0.57	0.52	1.17	0.89	1.82	1.10
Error in peak runoff (%)	3B41RT	0.38	25.00	4.72*	71.80*	91.50*	70.80*	110.5*	71.30*
	3B42RT	14.15	4.00	51.90*	70.40*	84.90*	71.90*	109.4*	27.20*
Error in peak runoff time (h)	3B41RT	0.0	0.0	0.0*	1.0*	0.0*	1.0*	0.0*	1.0*
	3B42RT	0.0	0.0	0.0*	0.0*	0.0*	0.0*	0.0*	0.0*
Error in runoff volume (%)	3B41RT	7.26	78.90	33.60*	7.80*	67.30*	0.42*	82.10*	2.80*
	3B42RT	28.30	67.00	1.60*	16.60*	18.50*	16.60*	31.70*	9.50*

* Computed from the simulation obtained from the mean of 200 realizations.

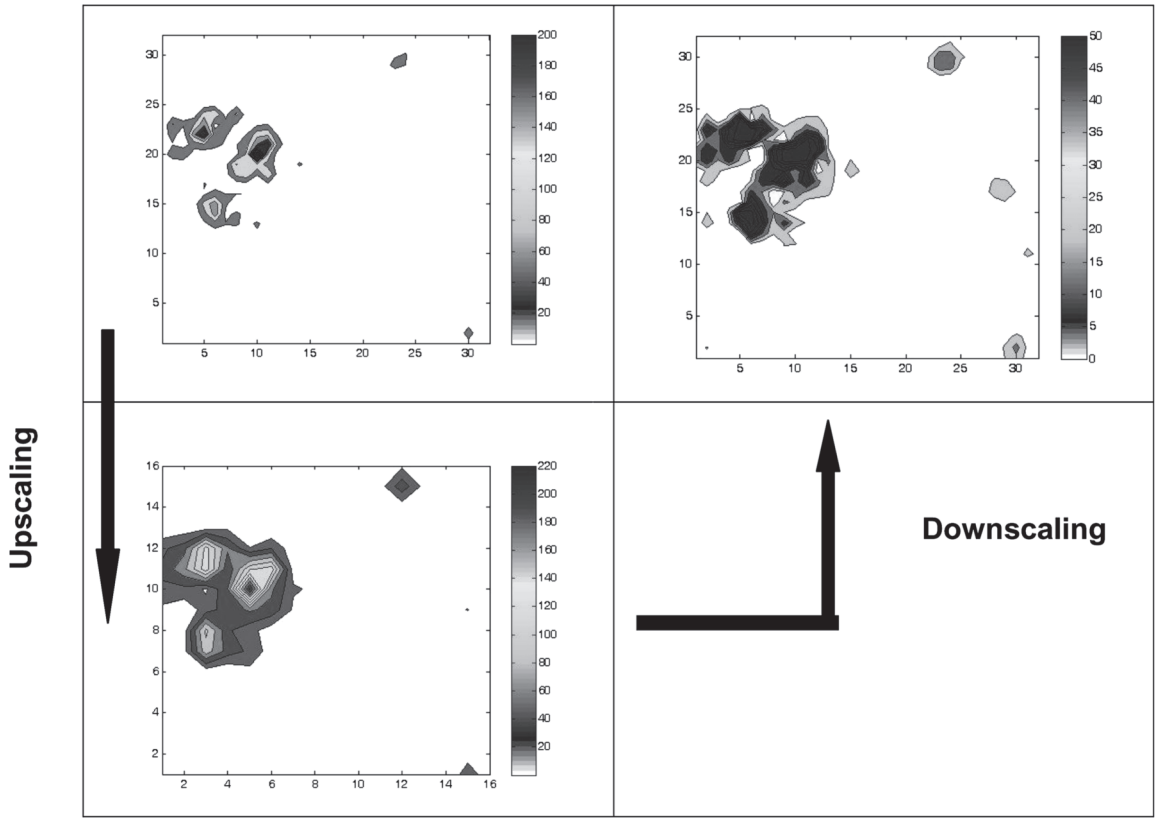

FIG. 10. Example of the random effect of spatial downscaling. A (top left) 32 × 32 rainfall field is upscaled to a (bottom left) 16 × 16 rainfall field. (top right) The downscaled 32 × 32 rainfall field from the corresponding 16 × 16 upscaled field is shown. Units for rainfall rates are mm h^{-1}. (Note that the mean rainfall intensity is strictly preserved during downscaling.)

distribution. Therefore, a more timely question is, how accurate is the spatial structure preservation of rainfall during downscaling and what does it mean for the simulation of overland runoff?

Hence, to gain further understanding of the implications of the uncertainty of satellite rainfall downscaling, a few subbasins are examined. These subbasins are located along the three main river reaches of the UC River basin (Fig. 1). Using the satellite product 3B42RT and the event 1, the purpose here is to relate the cumulative (in time) rainfall estimated by satellite at each disaggregated scale to the simulated cumulative runoff for the selected subbasins. In principle, this exercise allowed a closer look at the rainfall-runoff process using downscaled data at the subbasin level.

Figure 11 shows the cumulative rainfall for the selected subbasins as a function of disaggregated scale and location (upstream, midstream, and downstream) for one of the three river reaches (reach 2, see Fig. 1). The cumulative rainfall is calculated from the mean of the 200 MC downscaled realizations. Rather than achieving a strict conservation of rainfall volume at each scale, a considerable increase or decrease of cumulative rainfall volume is observed as the disaggregated scale decreases for a given subbasin (Fig. 11, top). Some subbasins experience an increase in rainfall volume, whereas others experience a decrease with downscaling. The offset in capturing the true rainfall volume widens consistently as scales become smaller. This clearly indicates that although a downscaling scheme may be constrained to preserve the rainfall intensity within a square domain of rainfall field, it can fail to do likewise for irregularly sized subbasins. (Refer back to Fig. 5 to gain a better grasp of each subbasin and the number of disaggregated satellite grid boxes that become available for estimation of areal averaged rainfall at each scale.) Figure 11 (bottom) shows the corresponding effect of downscaled satellite rainfall on runoff generation for the same set of selected subbasins along river reach 2. Comparison of the two panels (top and bottom) of Fig. 11 reveals that wherever rainfall is downscaled to a net higher amount, it usually results in a higher total runoff volume of the same subbasin. For certain subbasins, this effect appears dampened because of possibly drier antecedent moisture conditions. Generally, the scale effect is found to be more pronounced in runoff than it is

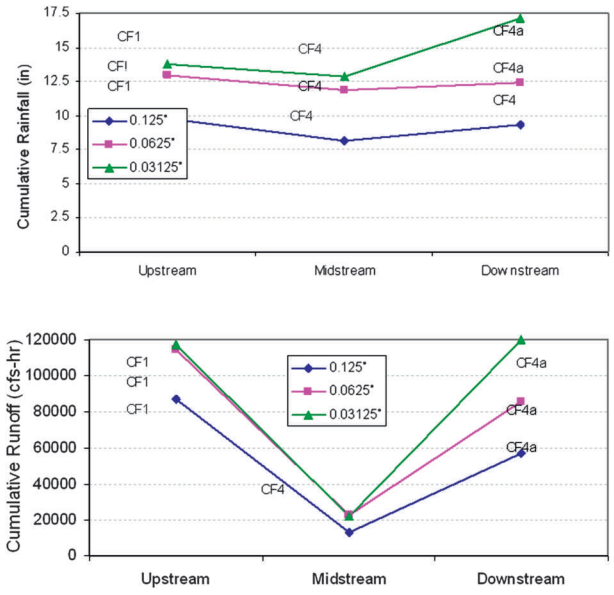

FIG. 11. Cumulative (top) rainfall (3B42RT) and (bottom) runoff along river reach 2 (Fig. 1) as a function of disaggregated scale and subbasin location (for event 1). The cumulative rainfall is calculated from the mean of 200 MC realizations, whereas runoff is derived from HEC-HMS. Terms CF1, CF4, CF4a, and so on are the HEC-HMS names for subbasins of the UC River basin shown in Fig. 1.

for rainfall as a result of the nonlinear thresholding and transformation of rainfall to runoff. Overland runoff is triggered either when the soil is completely saturated or when the rain rate exceeds the infiltration capacity of the soil. Table 5 summarizes the cumulative rainfall–runoff relationship as a function of downscaled resolution for the other two river reaches (1 and 3).

Finally, the rain rate histograms are shown in Fig. 12 for basin-averaged rainfall. For downscaled scenarios, we consider the mean of the 200 MC realizations for calculating the histograms. The most dramatic change in the statistical distribution of rain rates is found to occur at 0.125° (the first instance of downscaling from the native scale of 0.25°). A higher frequency of rain rates in the ranges of 1–5 mm h^{-1} is observed when compared to the native scale. This further explains why an increase in streamflow simulation uncertainty can be observed with downscaling. Overall, it is very clear from this closer inspection that the limitation of a chosen downscaling scheme in preserving the mean rainfall intensity over irregularly sized drainage units can result in an increase in simulation uncertainty as scales become smaller for a conceptual and semidistributed hydrologic model like HEC-HMS. We should point out that this limitation is manifested mainly because of the conceptual nature of the hydrologic model that requires averaging rainfall for irregularly sized drainage units from gridded data.

5. Conclusions

The objective of this study was to investigate spatial downscaling of satellite rainfall data for streamflow prediction for a medium-sized basin (~970 km^2) in Kentucky in anticipation of the proposed Global Precipitation Measurement (GPM) mission. Two TRMM-based real-time global satellite rainfall products were investigated: 1) the infrared (IR)-based 3B41RT product available at 1 hourly and 0.25° scales and 2) the combined microwave- and IR-based 3B42RT product available at 3 hourly and 0.25° scales. It was found that propagation of spatially downscaled satellite rainfall in the hydrologic model increased simulation uncertainty in streamflow as scales became smaller than 0.25°. The performance of the spatial downscaling scheme was not influenced by rainfall data type because similar performance was achieved with NEXRAD data. Although the downscaling scheme may preserve the rainfall intensity within the square rainfall field over which disaggregation is performed, the mean rainfall rate preservation is found not to be honored for irregularly sized subbasins. Closer inspection at the subbasin level confirmed that it was, indeed, this inability of the selected spatial downscaling scheme to preserve the

TABLE 5. Cumulative rainfall–runoff relationship as a function of downscaled resolution for subbasins along the river reach. HEC-HMS subbasin names are listed in parentheses in the column for rainfall.

	Upstream			Downstream	
	Scale (°)	Rainfall (in.)	Runoff (cfs h^{-1})	Rainfall (in.)	Runoff (cfs h^{-1})
River reach 1	0.125	2.6 (PF1)	20 000	11.4 (PF4d)	47 000
	0.0625	1.5 (PF1)	12 000	12.5 (PF4d)	57 000
	0.03125	1.1 (PF1)	9800	12.7 (PF4d)	56 000
River reach 3	0.125	8.0 (MF1)	104 000	9.5 (MF2b)	39 000
	0.0625	7.5 (MF1)	84 000	12.1 (MF2b)	57 000
	0.03125	6.8 (MF1)	87 000	10.4 (MF2b)	39 500

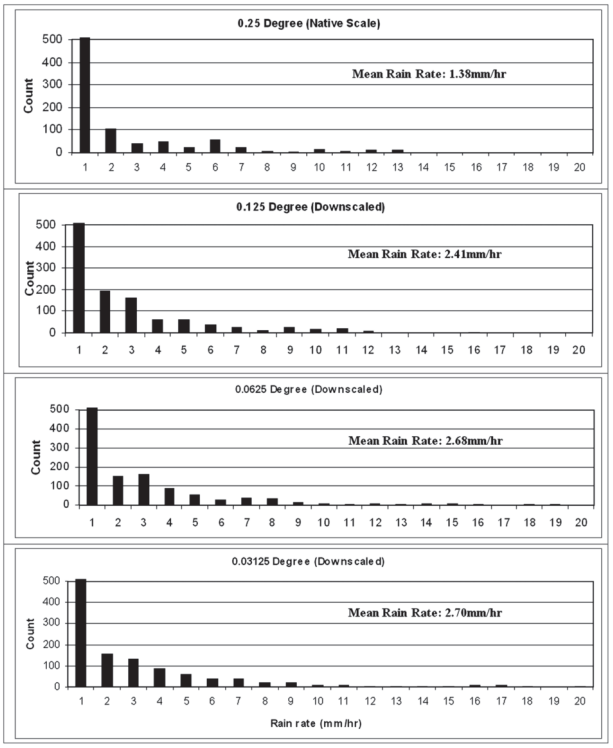

FIG. 12. The 3B42RT rain rate histograms for basin-averaged rainfall for (top to bottom) native scale, 0.125°, 0.0625°, and 0.03125°. For disaggregated scenarios, the histogram of the mean of 200 MC realizations is computed.

mean rainfall intensity that led to the increase in simulation uncertainty as scales became smaller.

This study is not without limitations. The spatial downscaling scheme used herein was a spatial disaggregation technique that did not leverage the space–time relationship of rainfall during the evolution of a storm event. Although the consideration of the mean of 200 MC realizations may be considered adequate to minimize the lack of storm persistence modeling, future extensions of this study should consider the more sophisticated variant of the Perica and Foufoula-Georgiou (1996b) scheme developed by Venugopal et al. (1999) where rainfall persistence is modeled during spatial downscaling. Also, because most spatial downscaling schemes are different in algorithm formulation, findings from this study are also limited to the particular scheme studied herein. In an earlier study, Ferraris et al. (2003) compared three conceptually different downscaling methods and reported that most downscaling techniques, despite the conceptual differences, have similar implications in streamflow prediction. Nevertheless, conclusions from this study should not be generalized for all spatial downscaling techniques currently available for disaggregation of satellite rainfall data.

This study is also conditioned on the specific hydrologic model used. HEC-HMS requires subbasin-averaged rainfall for simulation of runoff and streamflow, wherein, we have specifically observed that the rainfall average for irregularly sized subbasins is not conserved during downscaling. Grid-based distributed hydrologic modeling that requires no such averaging for subbasins are likely to yield more consistent results with downscaling (Bindlish and Barros 2000). The role played by hydrologic modeling in the transformation of downscaled rainfall to runoff is, therefore, an important topic for future studies. Given that many downscaling schemes leverage physical information on the storm systems [such as CAPE for Perica and Foufoula-Georgiou (1996b)], it is also important that future studies tackle the role played by the meteorological aspect of storms.

Findings from this study are important, because satellite-based estimates of precipitation are well known to increase in error complexity at smaller (hydrologically relevant) spatial scales (Hossain and Anagnostou 2006). Recently, PEHRPP has formulated an agenda to understand these hydrologically relevant features of satellite rainfall uncertainty and devise more pertinent error metrics. This work is currently in its nascent stages and depends on community feedback for advancement. In an earlier study, Hossain and Huffman (2008) have articulated three major dimensions of satellite rainfall uncertainty that should be part of any framework for building such error metrics: 1) temporal dimension (how does the error vary in time?); 2) spatial dimension (how does the error vary in space?); and 3) retrieval dimension (how ''off'' is each rainfall estimate from the true value over rainy areas?).

As the GPM era approaches, more coherent and higher-resolution rainfall data are being planned for the user community. Hence, there is an urgent need now to assess spatial downscaling along the three uncertainty dimensions. Such an effort can help devise optimal approaches for runoff generation over ungauged areas when satellite rainfall products are the sole source of rainfall. A natural extension of this study is, therefore, to investigate methods for developing a ''hybrid'' downscaling scheme that can leverage knowledge of scale-dependent uncertainty of satellite rainfall data (at the native scale) during spatial downscaling. For a user, it would be beneficial if hydrologically relevant uncertainty estimates for downscaled satellite rainfall data is projected by the downscaling scheme. These estimates could then provide guidance to the user on the level to which the downscaled data could be reasonably implemented in hydrologic models and the applications for which downscaled satellite data would be acceptable.

Acknowledgments. The corresponding author acknowledges the valuable insights on the wavelet-based spatial downscaling scheme provided by Dr. Efi Foufoula-Georgiou of the University of Minnesota. The code for downscaling was provided by Dr. Venu Venugopal of the Indian Institute of Science. Sayma Rahman was supported by the Selected Professions Fellowship from the American Association of University Women (AAUW). Supplemental support from the Center for Environmental Sciences and Engineering at the University of Connecticut was also provided to Rahman. Ling Tang was supported by the NASA Earth System Science Fellowship. Constructive comments from three anonymous reviewers, the editor, and Dr. George Huffman of NASA's Laboratory of Atmospheres and Space System Science Applications are gratefully acknowledged. This study (through Faisal Hossain) was also partially supported by the NASA Rapid Prototyping Capability Program (through the University of Mississippi) and the NASA New Investigator Program (Grant NNX08AR32G).

TABLE A1. Downscaling verification statistics.

Scale (°)	Mean (mm h^{-1})
0.25	0.0762
0.125	0.0762
0.0625	0.0762
0.03125	0.0762
0.015625	0.0762

APPENDIX

Verification of the Downscaling Scheme

a. Preservation of the mean

We first verified the Perica and Foufoula-Georgiou (1996b) downscaling scheme in terms of its ability to preserve the mean rainfall intensity over a 64 × 64 gridded domain using actual 3B42RT data. Table A1 and Figure A1 show the mean rainfall rate of 100 realizations as a function of downscaled resolution for a given rainfall distribution at the native scale of 0.25°.

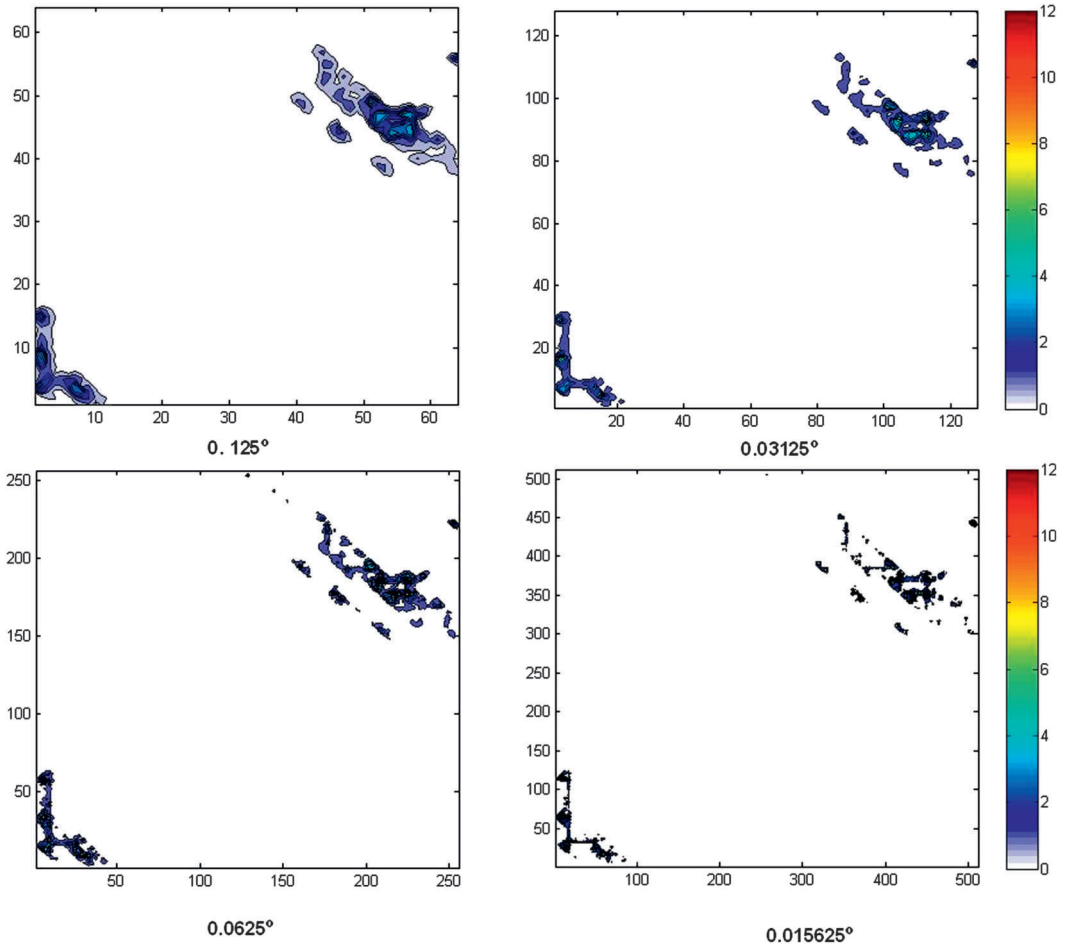

FIG. A1. Mean rainfall map from 100 realizations of downscaled 3B42RT data from a 64 × 64 gridded domain.

TABLE A2. Checking consistency of the downscaling scheme using fine-resolution data from NEXRAD and PERSIANN products (at 0.04°).

	NEXRAD		Satellite (PERSIANN)	
Spatial scale (°)	0.08°	0.04°	0.08°	0.04°
Correlation	0.9046	0.8092	0.9024	0.7809
Mean error (mm h^{-1})	−0.0030	−0.0572	−0.0011	−0.0144

Statistically, we found that the downscaling scheme also preserves the mean rainfall for each individual realization.

b. Checking consistency of downscaling

For checking consistency of the downscaling scheme, the satellite rainfall data product called PERSIANN and NEXRAD stage IV data available at 0.04° were used. First, the 0.04° data was aggregated up to 0.16° (via 0.08° and then 0.16°), then downscaled back to 0.08° and 0.04°. At each level of downscaling (0.08° and 0.04°), downscaled data were compared to true (non-downscaled) rainfall data at that scale to benchmark the similarity in the spatial distribution of downscaled data. Table A2 shows correlation and mean error (between downscaled and true nondownscaled data) at scales of 0.04° and 0.08°.

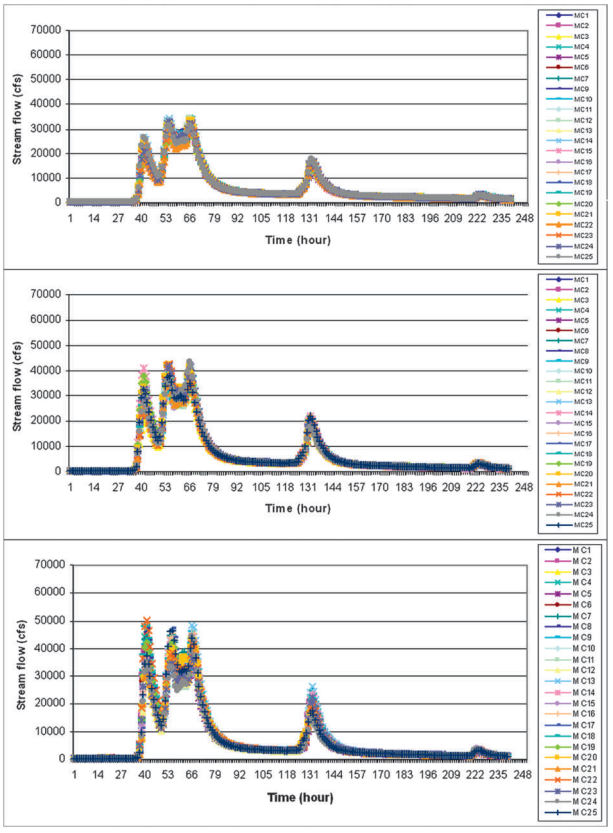

FIG. A2. Propagation of 25 downscaled MC realizations of 3B41RT for event 1 for (top to bottom) 0.125°, 0.0625°, and 0.03125°.

c. Equivalency of propagating mean ± σ through HEC-HMS

In the current scheme of operations, HEC-HMS lacks an automatic system for propagating multiple MC realizations of rainfall. Each realization needs to be propagated manually. Hence, we first propagated 25 MC realizations of downscaled 3B41RT for event 1 through HEC-HMS to verify if that would be closely equivalent to propagating only the mean and $\pm\sigma$ of the ensemble. Figure A2 shows the streamflow simulation for each of the 25 MC realizations for the downscaled resolutions of 0.125°, 0.0625°, and 0.03125°. It is clear that the spread of streamflow simulation is numerically very similar to that obtained from propagating the mean ± σ of 200 rainfall realizations (cf. with Fig. 8a).

REFERENCES

Ahrens, B., 2003: Rainfall downscaling in an alpine watershed applying a multiresolution approach. *J. Geophys. Res.,* **108,** 8388, doi:10.1029/2001JD001485.

Barry, D. A., and K. Bajracharya, 1995: On the Muskingum-Cunge flood routing method. *Environ. Int.,* **21,** 485–490, doi:10.1016/0160-4120(95)00046-N.

Bindlish, R., and A. P. Barros, 2000: Disaggregation of rainfall for one-way coupling of atmospheric and hydrological models in regions of complex terrain. *Global Planet. Change,* **25,** 111–132.

Ebert, E., J. E. Janowiak, and C. Kidd, 2007: Comparison of near real-time precipitation estimates from satellite observations and numerical models. *Bull. Amer. Meteor. Soc.,* **88,** 47–64.

Ferraris, L., S. Gabellani, N. Rebora, and A. Provenzale, 2003: A comparison of stochastic models for spatial rainfall downscaling. *Water Resour. Res.,* **39,** 1368, doi:10.1029/2003WR002504.

Fulton, R. A., J. P. Breidenbach, D.-J. Seo, D. A. Miller, and T. O'Bannon, 1998: The WSR-88D rainfall algorithm. *Wea. Forecasting,* **13,** 377–395.

Gaffin, D. M., and J. C. Lowery, cited 2008: A rainfall climatology of the NWSFO Memphis county warning area. NOAA Tech. Memo. NWS SR-175. [Available online at http://www.srh.noaa.gov/meg/rainclim.html.]

Harris, A., and F. Hossain, 2008: Investigating the optimal configuration of conceptual hydrologic models for satellite-rainfall-based flood prediction. *IEEE Geosci. Remote Sens. Lett.,* **5,** 532–536.

——, S. Rahman, F. Hossain, L. Yarborough, A. C. Bagtzoglou, and G. Easson, 2007: Satellite-based flood modeling using TRMM-based rainfall products. *Sensors,* **7,** 3416–3427.

HEC, 2000: Hydrologic Modeling System, HEC-HMS. U.S. Army Corps of Engineers, Hydrologic Engineering Center Tech. Reference Manual CPD-74B, 157 pp.

Hong, Y., K.-L. Hsu, S. Sorooshian, and X. Gao, 2005: Improved representation of diurnal variability of rainfall retrieved

from the Tropical Rainfall Measurement Mission Microwave Imager adjusted Precipitation Estimation From Remotely Sensed Information Using Artificial Neural Networks (PERSIANN) system. *J. Geophys. Res.,* **110,** D06102, doi:10.1029/2004JD005301.

——, R. F. Adler, F. Hossain, S. Curtis, and G. J. Huffman, 2007: A first approach to global runoff simulation using satellite rainfall estimation. *Water Resour. Res.,* **43,** W08502, doi:10.1029/2006WR005739.

Hossain, F., and E. N. Anagnostou, 2006: A two-dimensional satellite rainfall error model. *IEEE Trans. Geosci. Remote Sens.,* **44,** 1511–1522, doi:10.1109/TGRS.2005.863866.

——, and G. J. Huffman, 2008: Investigating error metrics for satellite rainfall at hydrologically relevant scales. *J. Hydrometeor.,* **9,** 563–575.

——, and D. P. Lettenmaier, 2006: Flood prediction in the future: Recognizing hydrologic issues in anticipation of the Global Precipitation Measurement mission. *Water Resour. Res.,* **44,** W11301, doi:10.1029/2006WR005202.

Huffman, G. J., R. F. Adler, D. T. Bolvin, G. Gu, E. J. Nelkin, K. P. Bowman, Y. Hong, E. F. Stocker, and D. B. Wolff, 2007: The TRMM Multisatellite Precipitation Analysis (TMPA): Quasi-global, multi-year, combined-sensor precipitation estimates at fine scales. *J. Hydrometeor.,* **8,** 38–55.

Janowiak, J., R. J. Joyce, and Y. Yarosh, 2001: A real-time global half-hourly pixel-resolution infrared datasets and its application. *Bull. Amer. Meteor. Soc.,* **82,** 205–217.

Kull, D. W., and A. D. Feldman, 1998: Evolution of Clark's unit graph method to spatially distributed runoff. *J. Hydrol. Eng.,* **3,** 9–19, doi:10.1061/(ASCE)1084-0699(1998)3:1(9).

Lin, Y., and K. E. Mitchell, 2005: The NCEP stage II/IV hourly precipitation analyses: Development and applications. Preprints, *19th Conf. on Hydrology,* San Diego, CA, Amer. Meteor. Soc., 1.2. [Available online at http://ams.confex.com/ams/Annual2005/techprogram/paper_83847.htm.]

Nash, J. E., and J. V. Sutcliffe, 1970: River flow forecasting through conceptual models part I—A discussion of principles. *J. Hydrol.,* **10,** 282–290.

Nijssen, B., G. M. O'Donnell, D. P. Lettenmaier, D. Lohmann, and E. F. Wood, 2001: Predicting the discharge of global rivers. *J. Climate,* **14,** 3307–3323.

Nykanen, D. K., E. Foufoula-Georgiou, and W. Lapenta, 2001: Impact of small-scale rainfall variability on larger-scale spatial organization of land–atmosphere fluxes. *J. Hydrometeor.,* **2,** 105–121.

Perica, S., and E. Foufoula-Georgiou, 1996a: Linkage of scaling and thermodynamic parameters of rainfall: Results from midlatitude mesoscale convective systems. *J. Geophys. Res.,* **101** (D3), 7431–7448.

——, and ——, 1996b: A model for multi-scale disaggregation of rainfall based on coupling meteorological and scaling descriptions. *J. Geophys. Res.,* **101** (D21), 26 347–26 361.

Rahman, S., 2008: Investigating effectiveness of spatial downscaling of satellite rainfall data for flood prediction. M.S. thesis, School of Engineering, University of Connecticut, 113 pp.

Shepherd, J. M., H. Pierce, and A. J. Negri, 2002: Rainfall modification by major urban areas: Observations from spaceborne rain radar on the TRMM satellite. *J. Appl. Meteor.,* **41,** 689–701.

Smith, E. A., and Coauthors, 2007: The international global precipitation measurement (GPM) program and mission: An overview. *Measuring Precipitation from Space: EURAINSAT and the Future,* V. Levizzani, P. Bauer, and F. J. Turk, Eds., Advances in Global Change Research, Vol. 28, Springer, 611–654.

Sorooshian, S., K. L. Hsu, X. Gao, H. V. Gupta, B. Imam, and D. Braithwaite, 2000: Evaluation of PERSIANN system satellite-based estimates of tropical rainfall. *Bull. Amer. Meteor. Soc.,* **81,** 2035–2046.

Troutman, T. W., M. A. Rose, L. M. Trapasso, and S. A. Foster, cited 2008: A Comprehensive Heavy Precipitation Climatology for Middle Tennessee. [Available online at http://www.srh.noaa.gov/bna/research/precip.htm.]

Venugopal, V., E. Foufoula-Georgiou, and V. Sapozhnikov, 1999: A space-time downscaling model for rainfall. *J. Geophys. Res.,* **104** (D16), 19 705–19 721.